Mon. Not. R. Astron. Soc. **000**, 000–000 (0000) Printed 7 January 2007 (MN LATEX style file v1.4)

Thermal Desorption of Water-Ice in the Interstellar Medium

Helen J. Fraser[1⋆†], Mark P. Collings[1], Martin R.S. McCoustra[1] and David A. Williams[2]
[1] *School of Chemistry, University of Nottingham, University Park, Nottingham, NG7 2RD, U.K.*
[2] *Department of Physics and Astronomy, University College London, Gower Street, London, WC1E 6BT, U.K.*

7 January 2007

ABSTRACT
Water (H_2O) ice is an important solid constituent of many astrophysical environments. To comprehend the role of such ices in the chemistry and evolution of dense molecular clouds and comets, it is necessary to understand the freeze-out, potential surface reactivity, and desorption mechanisms of such molecular systems. Consequently, there is a real need from within the astronomical modelling community for accurate empirical molecular data pertaining to these processes. Here we give the first results of a laboratory programme to provide such data. Measurements of the thermal desorption of H_2O ice, under interstellar conditions, are presented. For ice deposited under conditions that realistically mimic those in a dense molecular cloud, the thermal desorption of thin films (≈50 molecular layers) is found to occur with zero order kinetics characterised by a surface binding energy, E_{des}, of 5773 ±60 K, and a pre-exponential factor, A, of $10^{30\pm2}$ molecules cm^{-2} s^{-1}. These results imply that, in the dense interstellar medium, thermal desorption of H_2O ice will occur at significantly higher temperatures than has previously been assumed.

Key words: molecular data – molecular processes – methods: laboratory – ISM: molecules

1 INTRODUCTION

It has become clear over the last decade that purely gas phase schemes cannot account for the variety and richness of chemistry occurring in the interstellar medium (ISM), particularly in denser regions of molecular clouds where star formation is occurring. In such environments gas-grain interactions must also play a key role (Williams 1998). Within the lifetime of a dense molecular cloud (on the order of 10^6 yr), the grains accrete icy mantles as atomic and molecular species freeze-out onto the grains. The ices are processed further by cosmic ray impacts, UV photolysis, and shocks. Consequently, the chemical composition of these icy mantles is significantly different from that of the local gas phase environment (Rawlings 2000). During cloud collapse and stellar formation the grains are reheated, and molecules are recycled from the solid state into the gas phase environment. In regions where the H_2O concentrations are depleted it is assumed that the species is still locked in the icy mantles on the grains, and consequently, that the temperature is below the sublimation temperature of the tracer gas (van Dishoeck & van der Tak 2000). When evaluating these environments it is clearly necessary to understand the sublimation behaviour of the ice, and its thermal stability. The surface binding energy, E_{des}, and sublimation rates of molecular ices may only be obtained empirically. When combined, these data can be used to determine molecular residence times on the ice surface, in terms of a population half-life as a function of temperature. These data are also applicable in other astronomical environments, such as cometary nuclei and comae, planetary surfaces and satellites.

H_2O is the most abundant molecular ice in dense ISM regions (Ehrenfreund & Schutte 2000). The H_2O ice band at 3.07 μm is detected on lines of sight towards

⋆ The Raymond & Beverly Sackler Laboratory for Astrophysics, Sterrewacht Leiden, Leiden University, Postbus 9513, 2300 RA Leiden, The Netherlands.
† Corresponding author: The Raymond & Beverly Sackler Laboratory for Astrophysics, Sterrewacht Leiden, Leiden University, Postbus 9513, 2300 RA Leiden, The Netherlands fraser@strw.leidenuniv.nl

reddened stars that have a visual extinction above a critical value (Whittet 1993) and is typically one of the strongest bands in interstellar IR spectra. The abundance and morphology of H_2O ice in the ISM is generally inferred from the intensity and line profile of the 3.07 μm band. At low pressures and temperatures, such as those in the ISM, the H_2O ice can exist in both amorphous and crystalline forms. To further complicate the picture, the amorphous ice can exist in both high-density (1.1 g cm^{-3}) and low-density (0.94 g cm^{-3}) forms, reflecting differences in the porosity of the material, with a phase change from former to latter occurring irreversibly between 38 – 80 K (Jenniskens et al., 1995). It is generally assumed that the dominant morphology of icy mantles on interstellar grains resembles that of high density amorphous ice, with other 'impurity' molecules trapped in the H_2O ice matrix (Jenniskens et al. 1995). This is evident in comparisons of ISO SWS and ground based observations with laboratory spectra of mixed ice analogues (Ehrenfreund & Schutte 2000 and references therein). However, laboratory spectra of pure H_2O ices show clear differences in the line profile of the 3.07 μm feature associated with different ice morphologies and temperatures (Jenniskens et al. 1997). It is therefore likely that some H_2O ices have undergone 'mild processing' and re-cooling, (such as gentle heating below 80 – 100 K, or rapid localised heating due to shocks), and will therefore also exist in low-density amorphous and crystalline forms (Jenniskens & Blake, 1994, 1996). The physical properties of the H_2O ice, such as density, conductivity, vapour-pressure, and sublimation rate, are dictated by its structure. Significant differences are expected between the surface chemistry and bulk behaviour of the ice phases. In addition, the physical and chemical properties of the ice may also be affected by way the ice film is deposited, its lifetime, and processing prior to thermal desorption (Sack & Baragiola 1993).

This paper is the first in a series of papers reporting new experimental results on gas-surface interactions occurring under conditions resembling those in the ISM and star-forming regions. With the aid of a purpose-built instrument, we are now able, for the first time, to provide the astrochemical community with experimental results addressing not only desorption energies, but also sticking probabilities and desorption mechanisms. Here we present the results of laboratory studies to determine the surface binding energies on, and sublimation rates of H_2O ice under interstellar conditions. Previous studies, where the surface binding energies were determined from spectroscopic data, suggested that the surface binding energy of H_2O on H_2O ice was 4815 $\pm$15 K or 5070 $\pm$50 K, for unannealed and annealed ice samples respectively (Sandford & Allamandola 1988). It was also presumed that the desorption kinetics of the system were first order. These data have been used extensively in the astronomy literature, where it is now widely reported that under interstellar conditions H_2O can only exist in the solid phase below about 100 K (Hasegawa & Herbst 1993, Sandford & Allamandola 1993, Ehrenfreund & Schutte 2000). The direct techniques used to determine the surface binding energy in this work are described in §2. The results are detailed in §3. In these experiments the thermal desorption of thin H_2O ice films is found to occur with zero order kinetics characterised by a surface binding energy, E_{des}, of 5773 $\pm$60 K, and a pre-exponential factor, A, of $10^{30\pm2}$ molecules cm^{-2} s^{-1}. In §4, a comparison is made with previous results, from both thermodynamic and spectroscopic techniques and the astrophysical implications of this work are discussed, focusing on applications associated with dense molecular clouds. The conclusions are summarised in §5.

2 EXPERIMENTAL METHOD

The Nottingham Surface Astrophysics Experiment (NoSAE) was designed to measure surface binding energies and sticking probabilities empirically and accurately, recreating the harsh interstellar environment under controlled laboratory conditions. A much fuller description than can be given here is to be found elsewhere (Fraser, Collings & McCoustra 2001). Basically, the experiment consists of a stainless steel ultrahigh vacuum (UHV) chamber with an operating base pressure of 6×10^{-11} Torr. The primary constituent (¿90%) of this vacuum is H_2, providing very similar conditions with the experiment chamber as those found in the ISM. The chamber is equipped with an effusive gas deposition system, quadrupole mass spectrometer (QMS), FTIR spectrometer and a Quartz Crystal Microbalance (QCM). The QMS is used for temperature programmed desorption (TPD) experiments (see §2.2), the FTIR for reflection-absorption infrared spectroscopy (RAIRS), and the QCM for thin film mass determination. The grain mimic is an uncharacterised gold film surface, suspended at the end of a cryogenic cold finger, capable of reaching 7 K. The sample is radiatively heated from the reverse side by a halogen bulb. The sample temperature is measured using two E-type (Ni-Cr alloy vs. Cu-Ni alloy) and one KP-type (Au including 0.7% Fe vs. Chromel) thermocouples, positioned on or near to the sample. The temperature can be controlled to better than 0.5 K, and measured accurately within 0.25 K. The upper temperature range of the system is 350 K. The whole system is linked via DAQ, GPIB, and RS232 communications to a pair of PC's, which are used to co-ordinate and control data acquisition from various instruments on the experiment.

2.1 Deposition

H_2O was obtained *in situ* from a liquid H_2O sample that had been deionized, filtered for organic and inorganic solutes, and subjected to three freeze-thaw cycles under a vacuum of better than 1×10^{-7} Torr. H_2O ice films were deposited at a rate of *ca.* 10^{10} molecules s^{-1} on the gold film substrate held at a temperature of 10 K, from a quasi-effusive molecular beam of H_2O, directed at 5° to the surface normal. At such low temperatures and slow deposition rates ballistic deposition results in the formation of high-density amorphous ice. Exposure of the substrate to gaseous H_2O was varied between 1 and 100 Langmuir (L), (1 Langmuir is equivalent to 1×10^{-6} Torr s), and film mass was estimated using the QCM. An exposure of 20 L corresponded to a film mass of *ca.* 3.8×10^{-7} g, which equates to a surface number density of H_2O of 2.44×10^{16} molecules cm^{-2}, or a film thickness of *ca.* 0.03 μm, when proper account of the QCM sensor area is made.

2.2 Temperature programmed desorption

The sublimation characteristics of the H_2O films were measured by temperature programmed desorption (TPD). In this method a linear temperature ramp is applied to the sample and the rate of desorption is measured by monitoring the amount of adsorbate that desorbs into the gas phase as a function of temperature. Desorption is an activated process which takes place at a rate given by

$$R = -\frac{dN_S}{dt} = k_d N_S^m \tag{1}$$

where $N_S$is the number of adsorbed molecules on the surface in molecules cm^{-2}, m is the order of the reaction and k_d is the rate constant, given by

$$k_d = A\exp\left(-\frac{E_{des}}{k_B T}\right) \tag{2}$$

where A is the pre-exponential factor, E_{des} is the binding energy of a molecule on the ice surface in J, k_B is the Boltzmann constant and T is the ice temperature in K. For convenience, in this paper the surface binding energies are expressed as E_{des}/k_B, i.e. in K, and the units of A are determined from k_d, i.e. for $m = 1$, A is expressed in s^{-1}, and where $m = 0$, A is expressed in molecules cm^{-2} s^{-1}. Equation (1) can be rewritten, to reflect the TPD signal that is actually measured during the experiment, i.e.

$$-\frac{dN_S}{dT} = k_d\frac{N^m}{\beta} \tag{3}$$

where β is the heating rate, dT/dt. The recorded TPD signal peaks at some temperature maximum, T_d, which corresponds to the point at which the desorption rate from the surface is at a maximum, i.e. ($d^2N_S/dt^2 = 0$). The TPD spectra are collected at increasing initial surface coverages, using the same linear heating ramp in each case. To a first approximation, the surface binding energy, E_{des}, can then be calculated directly by substituting for $k_d$in equation (3) (using equation (2)), differentiating and equating to zero

$$\frac{E_{des}}{k_B T_d^2} = \frac{A}{\beta} m N_S^{m-1}\exp\left(-\frac{E_{des}}{k_B T_d}\right) \tag{4}$$

provided the pre-exponential factor, A, is known. In a first order desorption process, where $m = 1$, A is assumed to be around 10^{12} to 10^{13} s^{-1}, approximately the vibrational frequency of the weak bond between the adsorbate molecule and the surface. It is also possible to evaluate the order of the reaction from the TPD peak shape and peak maximum provided that the activation energy for desorption and pre-exponential factor remain constant as a function of surface coverage. In practice however, desorption may not occur in a single step, the surface binding energy can vary across binding sites on the surface or with surface coverage, and the pre-exponential factor, A, may differ by several orders of magnitude. A more rigorous result can be obtained by modelling the desorption system and using numerical fitting methods with a number of TPD spectra to evaluate the values of A and E_{des} (see Woodruff & Delchar 1986, Attard & Barnes 1998 for a more complete discussion).

In these experiments the ice layers were warmed at a rate of 0.02 K s^{-1} and the QMS, tuned to mass 18 (H_2O^+), was used to monitor the gas phase composition during desorption from the substrate. The QMS was operated in a line-of-sight configuration so that only molecules originating from the sample surface produced a signal at the detector (Fisher & Jones 1999). Sample coverages of 1, 2, 5, 10, 20, and 50 L (sub-monolayer to multilayer) were used. In all cases, no desorption was observed before 120 K and desorption was complete by 170 K.

3 RESULTS

Fig. 1 shows a sequence of TPD spectra for H_2O films deposited at 10 K, with increasing surface coverage. The spectra show the change in intensity of the mass 18 (H_2O^+) signal at the QMS as the sample is slowly heated. An intense, asymmetric peak is observed at *ca.* 140 K, associated with the desorption of the bulk ice film from the Au substrate. There is little or no change in the shape of the leading edge peak with increasing exposure. Furthermore, the peak temperature, T_d, increases monotonically with exposure. These observations are typical of TPD spectra in which the desorption process follows zero order kinetics, as illustrated by Fig. 2. The figure shows results from a series of (a) zeroth and (b) first order TPD simulations (based on equation

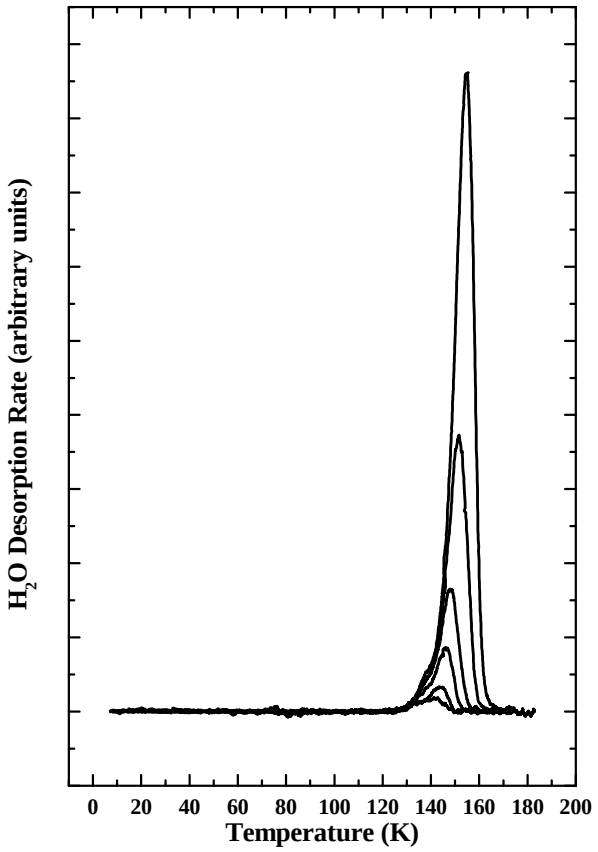

Figure 1: TPD spectra for H_2O ice films deposited at 10 K on a Au substrate. Spectra are shown for surface exposures of 1, 2, 5, 10, 20, and 50 L. See text for details.

3), at coverages of 2, 5, 10, 20, 50 and 100 monolayers of H_2O, and under conditions similar to those in this experiment. In the zeroth order case (Fig. 2 (a)), the TPD curves are asymmetric, with coincident rising edges, and the peak temperature, T_d, increases with exposure. This is typical of multilayer desorption, where the intensity of the TPD spectrum increases as more and more material is condensed onto the surface. The shift in T_d (the peak position) occurs because the desorption rate increases exponentially with temperature, so the rate can increase indefinitely until all the layers have been stripped away, and the TPD signal falls rapidly to zero. The bonding between the layers resembles that in a condensed solid of the adsorbate, so the desorption energy, E_{des}, and pre-exponential factor, A, are the same for every layer. In contrast, the first order desorption curves are symmetric about a single $T_d$value, independent of coverage (see Fig. 2 (b)). This closely resembles monolayer desorption kinetics, when the nature of the bonding between the adsorbate and the underlying substrate is clearly important. In a multilayer system (e.g. icy mantles on dust grains, or the ice system studied here) the monolayer is generally more tightly bound to the underlying substrate than the subsequent adsorbate layers. Consequently, the monolayer desorption peak appears at higher temperatures in the TPD spectrum than the multilayer desorption, reflecting a different E_{des} value. Its line shape profile will also differ, reflecting both a different Avalue, and the different reaction kinetics. A more complete discussion of this complex relationship between TPD line shape profiles, binding energies, and desorption kinetics can be found in Woodruff & Delchar (1986) or Attard & Barnes (1998). However, from a comparison between the experimental TPD spectra presented in Fig. 1 and the simulations in Fig. 2, it is reasonable to conclude that the results of this experiment are indicative of zeroth order kinetics. Furthermore, only a single peak is observed in the TPD spectra: even at low coverage it is not possible to deconvolve a monolayer desorption peak from the multilayer peak. Therefore no evidence exists to suggest that the desorption process is coverage dependant, nor that it is possible to distinguish between the multilayer and monolayer desorption processes. These observations are entirely consistent with previous reports on the TPD of ice from other hydrophobic, metal substrates (Kay et al. 1989; Dohnálek et al.1999, 2000).

In some cases, and particularly at higher exposure, a slight shoulder is observed on the leading edge of the 140 K TPD peak. Under these experimental conditions, the phase transition between amorphous and crystalline ice is known to occur between 120 and 140 K (Sack & Baragiola 1993). It might be expected therefore that all the desorbing ice should be in the crystalline phase by the time desorption occurs. However, given the relatively long timescale for this phase change (Dohnálek et al., 2000), it is likely that some desorption will occur from residual amorphous phase that has yet to undergo the phase change. The TPD peak of the amorphous ice will occur at a lower temperature than the main desorption peak since the vapour pressure of the amorphous ice is around three times greater than that of crystalline ice (Kouchi 1987). This behaviour is clearly illustrated in Fig. 3. Traces (a) and (b) show the TPD spectra from H_2O films of equivalent surface exposure, deposited at two temperatures, 10 and 100 K, producing high-density amorphous ice and low-density amorphous ice respectively. The films were cooled to 10 K and then treated as described in §2. Their TPD spectra are essentially equivalent, showing the amorphous ice desorption shoulder on the leading edge, which gradually flattens out as the crystallisation phase change dominates, and finally the major TPD peak, corresponding to desorption of the crystalline phase. Two further films, with double the surface coverage of the amorphous films, were also investigated. Trace (c) shows results for an H_2O film that was grown at 130 K then cooled to 10 K and warmed. The TPD spectrum from this ice film is narrower, with the onset of desorption occurring slightly later than the other spectra, and no evidence of the amorphous shoulder can be seen. These features are at-

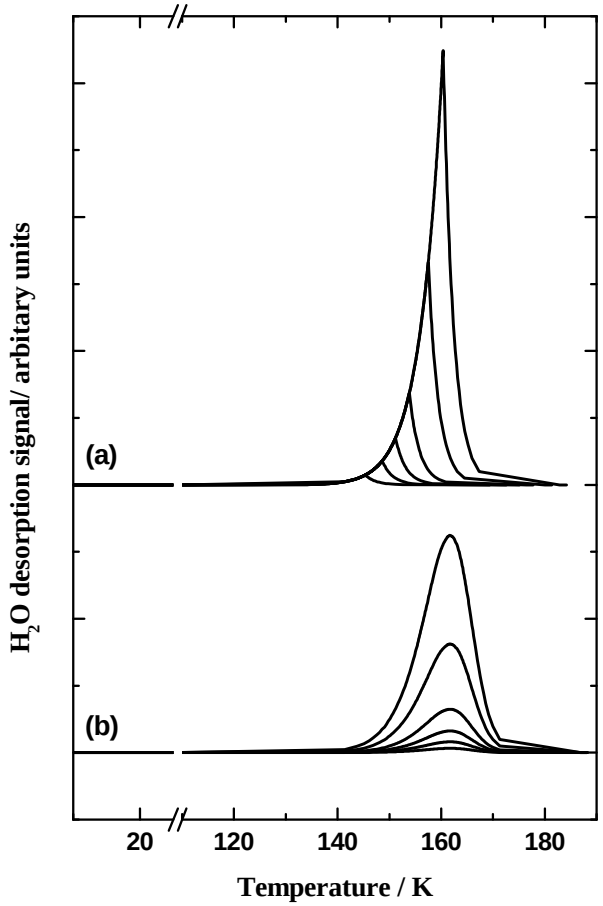

Figure 2: TPD spectra from a series of (a) zeroth ($A = 10^{30}$ molecules cm^{-2} s^{-1}) and (b) first order (A= 10^{13} s^{-1}) simulations (based on equation 3), at coverages of 2, 5, 10, 20, 50 and 100 monolayers of H_2O. In each case, the desorption energy, E_{des}, was fixed at 5773 K, and the heating ramp, β, was 0.01 Ks^{-1}.

tributed to the purely crystalline nature of this ice film. Finally trace (d) in this spectrum, was produced by depositing equal amounts of H_2O at 100 and then 10 K. The total surface coverage in (d) is therefore equivalent to (c). The TPD trace for this sample shows evidence of the amorphous phase desorption, but the phase change appears to be much faster than in (a) or (b), and spectrum is dominated by desorption from the crystalline phase. Similar results have been found in previous studies of ice desorption from various substrates, where the rate of crystallisation has also been determined (Speedy et al. 1996; Smith et al. 1996).

A kinetic model was used to evaluate the surface binding energy, E_{des}, and the pre-exponential factor, A, for the crystalline H_2O ice system. To model the kinetics of the bulk ice desorption, a simple reaction scheme was constructed to describe the desorption process

$$H_2O(s) \stackrel{k_d}{\rightarrow} H_2O(g) \quad (5)$$

$$H_2O(g) \stackrel{k_p}{\rightarrow} pump \quad (6)$$

where the concentration of $H_2O(s)$ is equivalent to N_S, the number of adsorbed molecules on the surface, and k_p is the pumping coefficient of H_2O in this system. A zero order rate equation, based on equation (1), was used to describe the desorption of molecules into the gas phase

$$\frac{d[H_2O(g)]}{dt} = k_d \quad (7)$$

The rate coefficient, k_d, is equivalent to that described in equation (2). A similar first order rate equation was used to describe equation (6)

$$\frac{d[H_2O(g)]}{dt} = -k_d[H_2O(g)] \quad (8)$$

The TPD spectrum then represents the temporal evolution of these coupled differential equations as the system temperature is raised in a linear manner. Using an initial H_2O ice surface density of 2.44×10^{16} molecules cm^{-2} (corresponding to a 20 L exposure),

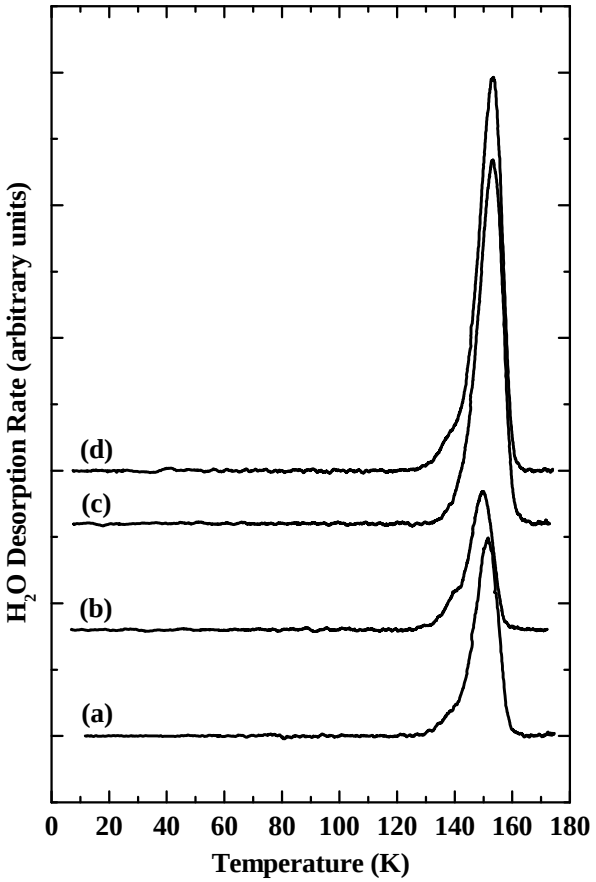

Figure 3: TPD spectra for H_2O ice films prepared (a) by 20 L exposure at 10 K, (b) by 20 L exposure at 100 K, (c) 80 L exposure at 130 K, and (d) 20 L exposure at 100 K followed by 20 L exposure at 10 K. Each film was then cooled to 10 K prior to desorption. For clarity, spectra are offset and only shown from 100 K.

an initial temperature of 10 K, and a linear temperature ramp of 0.02 K s^{-1}, model TPD spectra were calculated using a simple stochastic integration package*‡ (Houle & Hinsberg 1995) and compared with the empirical data. The unknown parameters in the model, the surface binding energy, E_{des}, and the pre-exponential for desorption, A, were then varied to best reproduce the empirical data. This was achieved for an A value of $10^{30\pm2}$ molecules cm^{-2} s^{-1} and an E_{des} value of 5773 $\pm$60 K. Fig. 4 shows the comparison of the model results with the empirical data.

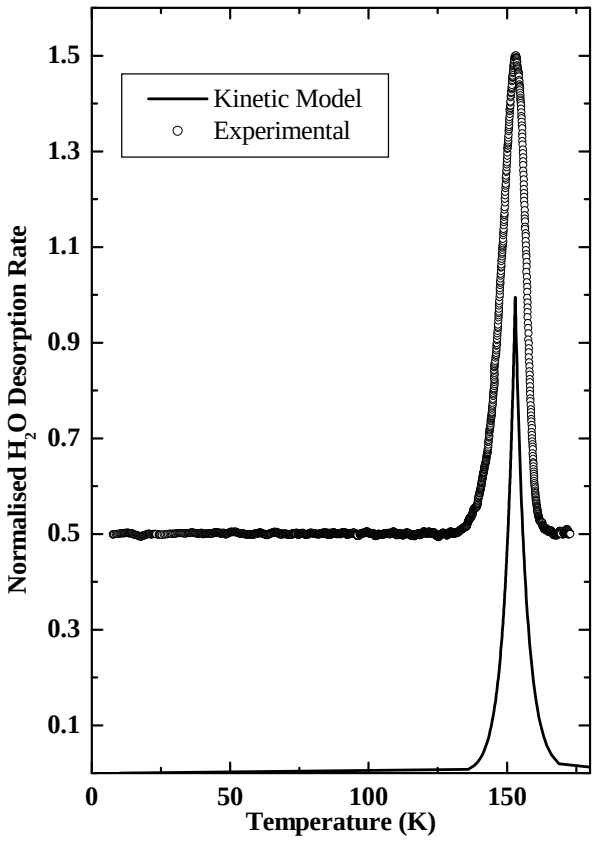

Figure 4: A comparison between experimental and modelled TPD spectra. See text for discussion.

It is much more complicated to evaluate the A and E_{des}values of the amorphous phase as the desorption and crystallisation processes are occurring simultaneously. To evaluate the gas phase H_2O concentration as measured in the experiment, it is necessary to couple equations describing the amorphous ice desorption rate and the crystallisation rate to equations (6) and (8). This work is currently ongoing, and will be the subject of a later paper. From the shapes and behaviour of the TPD curves in Fig.1 and Fig.3 however, it is clear that that the desorption mechanism for the amorphous ice is identical to that of the crystalline ice. Previous studies have drawn the same conclusion (Dohnálek et al., 1999, 2000). Initial results from our model suggest that the Afactor for amorphous ice is of the same order of magnitude, and that E_{des} is a few hundred K lower, than that of crystalline ice.

‡ * Chemical Kinetics Simulator, Version 1.0, IBM, IBM Almaden Research Centre, 1995. Further information may be obtained from the CKS website at http://www.almaden.ibm.com/st/msim/ckspage.html

4 ASTROPHYSICAL IMPLICATIONS

The results obtained here compare favourably with previous TPD measurements of H_2O desorption under UHV conditions, from a range of surfaces, (Kay et al. 1989; Haynes Tro & George 1992; Smith Huang & Kay 1997; Chakarov & Kasemo 1998; Dohnálek et al. 1999, 2000). When values for E_{des} and A are provided, the data are summarised in Table 1, where a comparison is also made with the spectroscopic results of Sandford & Allamandola (1988). With the exception of the latter results, the table clearly shows that for both ordered and disordered hydrophobic surfaces, the desorption energy and rate constant are independent of the substrate. In each case, the desorption kinetics resemble zero order rather than first order reaction kinetics.

None of the studies mentioned in Table 1 have identified any differences between the desorption of H_2O from H_2O layers and the desorption of H_2O from the underlying substrate. This indicates that H_2O is only weakly bound to hydrophobic substrates, and that the adsorbate-substrate binding energy is comparable to the adsorbate-adsorbate hydrogen bonding. In astrophysical terms, this indicates that the same desorption mechanism and desorption energy can be used to model H_2O desorption from any hydrophobic surface, (e.g. silicon, graphite). Similar desorption studies on hydrophilic surfaces (such as metal oxides, quartz, and silicates) indicate that H_2O bonds chemically to such surfaces. In such cases, the H_2O-substrate system exhibits alternative desorption kinetics, with even higher activation barriers (for example Stirniman et al. 1996; Trakhtenberg et al. 1997; Hudson et al. 2001). However, these systems do exhibit identical H_2O-H_2O desorption processes in the regime where the ice surface is substrate independent (i.e. the ice layer is thick enough that it is no longer influenced by the underlying substrate). Consequently, in ISM regions where relatively thick ice layers are formed, or the grain surface is hydrophobic, the underlying structure of the cosmic grain is not significant. Elsewhere, the grain material may influence the H_2O desorption mechanism. It will not be possible to say conclusively which H_2O desorption kinetics will dominate until the nature of interstellar grains has been clearly established.

As Table 1 shows, the results obtained in this study

(i) Crystalline Ice

Substrate	Au[a]	Ru (001) / Au (111)[b]	Sapphire[c]	CsI[d]
E_{des} (K)	**5773 ±60**	5803 ±96	5989	5070 ±50
A $\times 10^{30}$ (molecules cm^{-2} s^{-1})	**1**	4.58	2.8	$*2\times10^{12}$s^{-1}
m	**0**	0	0	1

(ii) Amorphous Ice

Substrate	Au[a]	Ru (001) / Au (111)[b]	Sapphire[c]	CsI[d]
E_{des} (K)	**5773 ±60**	5803 ±96	5989	5070 ±50
A $\times 10^{30}$ (molecules cm^{-2} s^{-1})	**1**	4.58	2.8	$*2\times10^{12}$s^{-1}
m	**0**	0	0	1

Table 1: A comparison surface binding energy, E_{des}, and pre-exponential factor, A, measurements for (i) crystalline ice and (ii) amorphous ice. * units in s^{-1} not molecules cm^{-2} s^{-1} as reaction was assumed to be first and not zero order. (a) This work, (b) Speedy et al. (1996), (c) Haynes et al. (1992), (d) Sandford & Allamandola (1988).

differ significantly from those obtained by Sandford & Allamandola 1988. Firstly, the E_{des} differs by *ca.* 800 K for both the crystalline and amorphous ice phases, and secondly the desorption kinetics in this study are clearly zero order and not first order. These two parameters are both significant when modelling interstellar environments, particularly when calculating the residence time of H_2O on interstellar grains, or establishing the ratio of solid to gas phase material.

Why do the two methods give such different results? The discrepancies must be related to the different assumptions that are made in interpreting the data under each set of experimental conditions. The most significant difference between the two experiments is that the spectroscopic data are taken under isothermal conditions at base pressures of *ca.* 2×10^{-8} Torr, whereas the TPD spectra are recorded in dynamic conditions at base pressures of 6×10^{-11} Torr. In the spectroscopic measurements, it was assumed that a first order rate law applied, and the value of $E_{des}$was determined indirectly, by monitoring the relative change in integrated intensity of a surface IR spectroscopic feature during isothermal desorption. Contrary to the assumptions made in Sandford & Allamandola's method, close to the desorption temperature, the sticking probability of H_2O molecules on the surface is no longer unity, and over the time period of the experiment it is possible for re-adsorption to occur, both from vacuum contaminants and desorbing gas. The evaluation of isothermal measurements is also complicated by non-equilibrium effects, including both crystallisation and re-adsorption. In the TPD experiments it is possible to obtain information on the order of the reaction and E_{des} directly, from the shape and position of the TPD curve. In UHV systems designed for TPD experiments, the pumping speed is so high that surface re-adsorption is not relevant. Unlike the spectroscopic data, the TPD spectra clearly show that crystallisation and desorption are occurring concurrently in the system. It is possible however to identify the amorphous, crystalline and 'phase change' regions of the TPD spectra from each other. With careful film preparation it is even possible to force the TPD spectrum to exhibit only crystalline behaviour, as was seen in Fig. 3. Furthermore, Kay and co-workers have made a number studies using TPD methods to determine the rates of crystallisation and desorption when they are occurring at the same time, and have found no significant difference between the desorption rates they measure

Grain T (K)	Half-life, $t_{1/2}$, (yr.)							
	Zero order desorption kinetics, i.e. $t_{1/2} = \frac{N_{S,0}}{2k_d}$ where $N_{s,0}$=1.15×10^{17} molecules cm^{-2}				First order desorption kinetics, i.e. $t_{1/2} = \frac{\ln 2}{k_d}$			
	H_2O on crystalline ice		H_2O on amorphous ice		H_2O on crystalline ice		H_2O on amorphous ice	
	(a)	(b)	(a)	(b)	(c)	(d)	(c)	(d)
10	**8.8×10^{231}**	*1.3×10^{200}*	**6×10^{224}**	*8.9×10^{188}*	4.6×10^{232}	*6.8×10^{200}*	3.8×10^{225}	*5.7×10^{189}*
20	**8.6×10^{105}**	*1×10^{90}*	**2×10^{102}**	*2.5×10^{84}*	4.5×10^{106}	*5.5×10^{90}*	1.3×10^{103}	*1.6×10^{85}*
30	**8.5×10^{63}**	*2.1×10^{53}*	**3×10^{61}**	*3.5×10^{49}*	4.5×10^{64}	*1.1×10^{54}*	2×10^{62}	*2.2×10^{50}*
40	**8.4×10^{42}**	*9.3×10^{34}*	**1.2×10^{41}**	*1.3×10^{32}*	4.4×10^{43}	*4.9×10^{35}*	7.6×10^{41}	*8.3×10^{32}*
50	**2.1×10^{30}**	*9.1×10^{23}*	**6.7×10^{28}**	*4.5×10^{21}*	1.1×10^{31}	*4.8×10^{24}*	4.3×10^{29}	*2.9×10^{22}*
60	**8.4×10^{21}**	*4.2×10^{16}*	**4.6×10^{20}**	*4.9×10^{14}*	4.4×10^{22}	*2.2×10^{17}*	2.9×10^{21}	*3.1×10^{15}*
70	**8.4×10^{15}**	*2.4×10^{11}*	**6.7×10^{14}**	*5.1×10^{9}*	4.4×10^{16}	*1.3×10^{12}*	4.3×10^{15}	*3.3×10^{10}*
80	**2.7×10^{11}**	*2.8×10^{7}*	**2.8×10^{10}**	*9.4×10^{5}*	1.4×10^{12}	*1.5×10^{8}*	1.8×10^{11}	*6.1×10^{6}*
90	**8.4×10^{7}**	*2.4×10^{4}*	**1.1×10^{7}**	*1.2×10^{3}*	4.4×10^{8}	*1.3×10^{5}*	7.2×10^{7}	*7.5×10^{3}*
100	**1.3×10^{5}**	*8.7×10^{1}*	**2.1×10^{4}**	*5.6×10^{0}*	7×10^{5}	*4.6×10^{2}*	1.4×10^{5}	*3.6×10^{1}*
110	**6.8×10^{2}**	*8.7×10^{-1}*	**1.3×10^{2}**	*7×10^{-2}*	3.6×10^{3}	*4.6×10^{0}*	8.1×10^{2}	*4.5×10^{-1}*
120	**8.4×10^{0}**	*1.8×10^{-3}*	**1.8×10^{0}**	*1.9×10^{-2}*	4.1×10^{1}	*9.8×10^{-2}*	1.1×10^{1}	*1.2×10^{-2}*
130	**2×10^{-1}**	*7.2×10^{-4}*	**4.7×10^{-2}**	*8.3×10^{-5}*	1.1×10^{0}	*3.8×10^{-3}*	3.1×10^{-1}	*5.3×10^{-4}*
140	**8.4×10^{-3}**	*5.9×10^{-6}*	**2.1×10^{-3}**	*4.5×10^{-5}*	4.2×10^{-2}	*2.3×10^{-4}*	1.4×10-2	*3.8×10^{-5}*
150	**5.3×10^{-4}**	*4×10^{-6}*	**1.5×10^{-4}**	*6×10^{-7}*	2.8×10^{-3}	*2.1×10^{-5}*	9.4×10^{-4}	*3.8×10^{-6}*

Table 2: The half-life, $t_{1/2}$, of H_2O molecules on H_2O ice surfaces as a function of temperature under zero and first order kinetics. In each case, the half-life is defined in the table, and represents the time it takes for the surface population of H_2O molecules on an interstellar grain to decrease to one half of its initial value. (a) E_{des} and A taken from this work, (b) E_{des} taken from Sandford & Allamandola (1988), A taken from this work, (c) E_{des} taken from this work, A taken from Sandford & Allamandola (1988), (d) E_{des} and A taken from Sandford & Allamandola (1988)

isothermally or dynamically (Speedy et al. 1996; Smith et al. 1996; Dohnálek et al. 1999, 2000). Finally the experimental conditions under which the TPD spectra were obtained most closely resemble those in the interstellar medium. We therefore believe that these data represent the parameters for H_2O that should be employed in astronomical models.

Table 2 shows the effect these new parameters have on the 'residence times' of H_2O molecules on H_2O ices and hydrophobic surfaces. It is not possible to define a residence time for a zero order process that is directly comparable (with the same units) with a first order process. Consequently, the results are presented here in terms of the half-life of the H_2O surface population, rather than the 'residence time, $1/k_d$' that is commonly used in the astronomical literature. The respective half-life values are defined in the table. It is important to note that the half-life of a zero order process also depends on the surface concentration of H_2O molecules. In these calculations this value was fixed at 1.15×10^{17} molecules cm^{-2}, equivalent to around 100 monolayers of H_2O ice, i.e. the number of H_2O layers expected to accrete on a interstellar grain during the lifetime of a dense cloud (Hasegawa & Herbst 1993). The half-lives calculated using the zero order $A$and E_{des} values obtained in this work are given in column one (crystalline ice) and three (amorphous ice).The results are also compared to half-life calculations using the data from Sandford & Allamandola (1993). The half-lives calculated using Sandford & Allamandola's first order $A$and E_{des} values are given in columns six (crystalline ice) and eight (amorphous ice). From Table 2 it is immediately clear that H_2O can remain on the grain surface at significantly higher temperatures than has previously been assumed, typically around 110 - 120 K rather than 90 - 100 K.

5 CONCLUSION

The surface binding energy and desorption kinetics of amorphous and crystalline H_2O ice have been studied under conditions similar to those found in denser regions of interstellar clouds. These data have been used to calculate the residence times of H_2O on H_2O and hydrophobic surfaces as a function of temperature. The results imply that, in the dense interstellar medium, thermal desorption of H_2O ice will occur at significantly higher temperatures, and different rates, than previously had been assumed. These data are of fundamental importance in the chemical modelling of many astrophysical environments. The effects may be particularly pronounced in so-called hot cores, which are very dense clumps of gas, remnants of a collapsing cloud that formed a massive star. Irradiation of the clumps heats the cores to temperatures in the range 100 - 300 K, when the ices evaporate, populating the gas with water and other trace molecules (cf. Millar 1993). The temperature of the evaporation may be crucial to relating the observed chemistry of hot cores to the implied rate of warming of the central star (Viti and Williams 1999).The results provide the astronomical community with reliable thermodynamic data pertaining to the desorption of H_2O under interstellar conditions.

ACKNOWLEDGEMENTS

The authors thank PPARC for their financial support, without which these experiments would not have been possible.

REFERENCES

Attard G., Barnes C., 1998, Surfaces, Oxford University Press, Oxford, UK
Chakarov D., Kasemo B., 1998, Phys. Rev. Lett., 81, 5181
Dohnálek Z., Ciolli R.L., Kimmel G.A., Stevenson K.P., Smith R.S., Kay B.D., 1999, J. Chem. Phys. 110, 5489
Dohnálek Z., Ciolli R.L., Kimmel G.A., Stevenson K.P., Smith R.S., Kay B.D., 2000, J. Chem. Phys. 112, 5932
Ehrenfreund P., Schutte W.A., 2000, in Minh Y.C., van Dishoeck E.F., eds, Astrochemistry: From Molecular Clouds to Planetary Systems, I.A.U., 197, p.135
Fisher C., Jones R.G., 1999, Surf. Sci, 424, 127
Fraser H.J., Collings M.P., McCoustra M.R.S., 2001, Rev. Sci. Inst., preprint submitted
Hasegawa T.I, Herbst E., 1993, MNRAS, 261, 83
Haynes D.R., Tro N.J., George S.M., 1992, J. Phys. Chem., 96, 8502
Houle F.A., Hinsberg W.D., 1995, Surf. Sci. 338, 329
Hudson P.K., Foster K.L., Tolbert M.A., George S.M., Carlo S.R., Grassian V.H., 2001, J. Phys. Chem. A, 105, 694
Jenniskens P., Blake D.F., 1994, Science, 265, 753
Jenniskens P., Blake D.F., 1996, ApJ, 473, 1104
Jenniskens. P, Blake D.F., Wilson M.A., Pohorille A., 1995, ApJ, 455, 389
Jenniskens. P, Banham S.F., Blake D.F., McCoustra M.R.S, 1997, J. Chem. Phys., 107, 1232
Kay B.D., Lykke K.R., Creighton J.R., Ward S.J., 1989, J. Chem. Phys. 91, 5120
Kouchi A., 1987, Nature, 330, 550
Millar, T. J. 1993, in Millar T. J., Williams D. A., eds., Dust and Chemistry in Astronomy, IoP Publishing, Bristol, p249
Rawlings J.M.C., 2000, in Minh Y.C., van Dishoeck E.F., eds, Astrochemistry: From Molecular Clouds to Planetary Systems, I.A.U., 197, p.15
Sack N.J., Baragiola R.A., 1993, Phys. Rev. Lett., 48, 9973
Sandford S.A., Allamandola L.J., 1988, Icarus, 76, 201
Sandford S.A., Allamandola L.J., 1993, ApJ, 417, 815
Smith R.S., Huang C., Wong E.K.L., Kay B.D., 1996, Surface Science, 367, L13
Smith R.S., Huang C., Kay B.D., 1997, J. Phys. Chem. B, 101, 6123
Speedy R.J., Debenedetti P.G., Smith R.S., Huang C., Kay B.D., 1996, J. Chem. Phys., 105, 240
Stirniman M.J., Huang C., Smith R.S., Joyce S.A., Kay B.D., 1996, J. Chem. Phys., 105, 1295
Trakhtenberg S., Naaman R., Cohen S.R., Benjamin I., 1997, J. Phys. Chem. B, 101, 5172
van Dishoeck E.F., van der Tak F.F.S., 2000, in Minh Y.C., van Dishoeck E.F., eds, Astrochemistry: From Molecular Clouds to Planetary Systems, I.A.U., 197, p.97
Viti S., Williams D. A., 1999, MNRAS, 305, 755
Whittet D.C.B., 1993, in Millar T.J., Williams D.A., eds, Dust and Chemistry in Astronomy. IOP Publishing, Bristol, p. 9
Williams D.A., 1998, Faraday Discuss., 109, 1
Woodruff D.P., Delchar T.A., 1986, Modern Techniques of Surface Science, Cambridge Univ. Press, Cambridge, UK